IDENTIFICATION OF STRESS INDUCED NUCLEATION SITES FOR MARTENSITE IN Fe-31.8wt%Ni-0.02wt%C ALLOY

Y. Sano, S. N. Chang, M. A. Meyers, and S. Nemat-Nasser

Center of Excellence for Advanced Materials
University of California, San Diego
La Jolla, CA

ABSTRACT

A novel plate impact recovery technique has been used to study the incubation time, the inception, and the initiation and growth of martensitic transformations in an Fe-31% Ni-0.02% C alloy, at a temperature of M_s + 10° C. The technique allows subjecting the sample to a single tensile pulse of pre-assigned duration and amplitude. The amplitude of the tensile pulse sufficient to induce transformation at the test temperature, was about 1.5 GPa. For a tensile pulse duration of 80ns, martensitic transformation was observed to have been initiated, but no fully transformed martensite lenses were produced. For a tensile pulse of 105ns duration, in addition to small incompletely grown lenses, fully grown martensite lenses were observed. The majority of these martensite lenses abutted the annealing twin boundaries, suggesting that these boundaries are favored nucleation sites for tensile stress wave-induced martensite in the system under investigation.

1. INTRODUCTION

Martensitic transformation can be induced at temperatures above M_s (martensite start), by tensile hydrostatic stresses which activate the dilatational component of the transformation strain, resulting in an interaction energy which favors the transformation. The interactions between the compressive, tensile,and shear stresses and the martensite transformations were investigated by Patel and Cohen [1], and Meyers and Guimaraes [2]. More recently, the normal plate impact technique has been used by Thadhani and Meyers [3] and Chang and Meyers [4]. These experiments showed that martensitic transformation can be induced by hydrostatic tensile pulses of sufficient amplitude and duration. The majority of the martensite lenses observed in experiments reported in [3,4] were fully grown, with their midribs extending from obstacle to obstacle within the grains. Thus, the initiation sites for transformation were not identified, nor were the incubation time and growth pattern established.

Recently, a novel technique has been developed at the University of California, San Diego, where, in a normal plate impact experiment, the sample can be subjected to a single tensile stress pulse of pre-assigned duration and amplitude, and then recovered for post-test characterization; see Ramesh et al. [5] and Sano [6]. We have used this technique to induce martensitic transformation at a temperature of M_s + 10°C, by tensile stress pulses of 1.5 GPa, and durations insufficient for the full growth of martensite lenses. In this manner, we have established the existence of an incubation time of somewhat less than 80ns, for the considered alloy. Furthermore, we have captured martensite lenses at early stages of growth, emanating from annealing twin boundaries.

2. EXPERIMENTAL PROCEDURES

Specimen Preparation

An Fe-31.8wt%Ni-0.02wt%C alloy was used in this investigation. It was cold-rolled to a thickness of 6.6mm from an initial thickness of 15.2mm. Subsequent to cold working, the material was annealed at 1100°C for 2 hours, yielding a grain size, as measured by the mean linear intercept, of 60 μm. The M_s temperature of this alloy, measured by the resistometric method during continuous cooling, was found to be -40°C. The specimens (for impact targets) were machined out of the plate into discs of 25.4mm diameter and about 1.6mm thickness. The disc-shaped specimens were mounted by the shrink fit method in a ring of AISI 304 stainless steel which has a shock impedance similar to the Fe-Ni alloy. The ring plays a role in minimizing the effects of lateral release waves.

The flyer plate was machined from a plate of 0.8mm thickness into a disc of 41.3mm diameter. For the flyer plate, AISI 1095 spring steel was used to ensure that only elastic deformation (in the flyer plate) would take place. Upon impact, the back momentum trap of 304 stainless steel had a thickness of 1.4mm and a diameter of 31.8mm. All the above discs were well lapped with diamond and oil. The flatness was checked with an optical flat under green light having a wave length of 5.4×10^{-4} mm, and was assured to be within one wavelength.

Impact Configurations

Experiments were performed both without a momentum trap, referred to as Setup I, and with a momentum trap including a gap, referred to as Setup II. Setup I was used to establish the required stress amplitude for transformation, and to reconfirm the previously obtained results of [3,4]. The new Setup II was then used to establish the nucleation and growth process, and to capture martensite lenses at various stages of growth. In this latter setup, a back momentum trap is used in conjunction with a flyer plate and a target. A small gap was provided between the target and the back momentum trap. A complete target assembly is shown in Fig. 1. In our experiments, a back momentum trap was glued on the rear side of the

target, with gaps of 7.5 and 10μm. The gaps are provided by positioning small segments of nickel sheet of desired thickness at four points between the target and the momentum trap. An iron-constantan thermocouple was glued onto the rear side of the specimen. The target assembly was then mounted within a phenolic disc holder. A coil of copper tubing was set on the edge of the rear side of the ring, through which liquid nitrogen was circulated for temperature control. An acrylic plate disc with screws for the tilting system, was attached to the back side of the phenolic disc holder. In Fig. 2 the propagation of the stress pulses into the target flyer plate and the momentum trap is sketched. Upon impact, compressive pulses are generated, both in the flyer plate and the target. The pulse in the flyer plate reflects back as a tensile release wave from the free surface of the flyer, and reaches the interface between the flyer and the target after a time interval of OP_2 which defines the total compressive pulse duration. The compressive pulse in the target is reflected off the gap as a tensile release pulse, until the gap is closed. It is then transmitted into the momentum trap. By adjusting the size of the gap, the duration of the tensile pulse can be controlled. Once this tensile release pulse passes the tail of the main compressive pulse in the target, it subjects the target to a tensile stress of pre-assigned amplitude and duration, the amplitude being controlled by the speed of the flyer and the duration by the size of the gap and the speed of the flyer. This tensile pulse is then reflected back from the interface between the target and the flyer plate as compression, and is transmitted into the momentum trap, as shown in Fig. 2. Shortly after, the tension, which reflects off the free face of the momentum trap, reaches the interface with the target, and the momentum trap separates, carrying with it the entire impact momentum. The target and the flyer remain essentially unmoved and are recovered for post-test analysis.

Gas Gun Setup

A gas gun (59mm diameter) was used to accelerate the flyer plate, glued to the front plate of a projectile to impact a target; nitrogen was used as the driving gas. Both the barrel and the chamber were evacuated in order to avoid producing a strong air shock ahead of the projectile which could disturb the target assembly. The impact velocity of the projectile was measured by three magnetic speed sensors placed at 12.5mm intervals, at the exit end of the barrel. Each sensor produces a signature of the event, namely the passage of the projectile. The tests were

conducted at -30° C, and a normal cooling rate of -1° C per minute was used for the target assembly.

3. RESULTS AND DISCUSSION

A summary of gas gun operating conditions and impact results is listed in Table 1. It was observed that no transformation occurred in the target specimen impacted at 1.4 GPa, while the targets impacted at 1.6 GPa (245ns) tensile pulse duration) showed martensitic transformation. The transformation product is localized in the center of the target specimens, as seen in Fig. 3. This non-uniform martensitic distribution agrees with the distribution of the tensile stresses throughout the target thickness. The duration of the tensile pulse is maximum in the interior of the target, in a region determined by the thickness ratio of the flyer plate and the target, and the gap between the target and the back momentum trap. The distance-time plot of Fig. 2 predicts the tensile stress history as a function of position. As the pulse duration is decreased from 105ns to 80ns, the extent of transformation and morphology of the martensite lenses are drastically altered. For Setup I with no momentum trap and with a 245ns pulse duration, the majority of the lenses are fully grown, i.e., they extend from barrier to barrier (Fig. 3). These barriers are, for the most part, grain boundaries and other lenses. Thus, one cannot determine the nucleation region for the transformation. With the new Setup II and a single pulse of 80ns duration, on the other hand, no fully transformed martensite lenses are observed; Fig 4(a). The plates have an average length of 4 μm, in contrast with the plates in Fig. 3 which have an average length of 60 μm.

One concludes from the above that the time (80ns) was not sufficient, under the imposed conditions, for the full growth of the lenses. These small, incompletely grown lenses are also present in the specimen tested at 105ns, in association with fully grown lenses (Fig. 4(b)). This condition is intermediate between the two well-defined cases: 245 and 80ns. The increase in the fraction of transformed material, with increasing pulse duration, confirms the isothermal nature of athermal martensitic transformation in Fe-Ni-C alloys [3]. As shown in Figs. 5(a) and (b), these incompletely grown lenses in the specimens have a high length-to-diameter ratio, and are always found to adjoin annealing-twin and grain boundaries.

The reasons why annealing twin boundaries are favored nucleation sites are not fully understood. It is interesting that Magee [7] reports the same association of martensite lenses first formed with annealing twins. So do Yeo [8] and Breedis [9]. These very small plates were thermally produced and preceded overall transformation. In the present research, the lenses are stress assisted, but the confirmation that annealing twins are preferential nucleation sites is strong evidence that the same mechanism is responsible for the nucleation of thermally- and stress-assisted martensite. Small (a few atomic layers thick) semi-coherent steps at coherent annealing twins would be the logical sites for nucleation, because of the presence of defects; models composed of special partial dislocation arrays have been proposed [10, 11]. A glissile semi-coherent twin boundary in which dislocation dissociation would occur could produce the steps required for nucleation. However, further evidence has to be obtained in order to fully characterize these sites.

It is instructive to calculate a propagation distance for a martensite lens in the 80ns time, assuming a 1,500 m/s velocity reported by Olson and Cohen [12] for an Fe-31%Ni alloy. The distance that a lens could propagate in this time interval is 120 μm. The fact that the lenses have only a fraction of that length is indicative of an incubation time for transformation, in agreement with nucleation theory. The partially grown lenses observed in Figs. 6(a) and (b) tend to occur symmetrically with respect to the boundary. This morphology is known, in fully grown lenses, as "butterfly".

4. CONCLUSION

Tensile stresses induced by the reflection of elastic stress waves off free surfaces, induce martensitic transformation in an Fe-31.8wt%Ni-0.02wt%C alloy at a temperature 10° C above the zero stress M_s. The martensite transformed is localized in a specific region which corresponds to the position of maximum tensile pulse duration. By providing a momentum trap behind the target, and a preset gap between the specimen and the momentum trap, the specimen is subjected to a single short tensile pulse, and then recovered. With a short single tensile pulse of duration of the order of 100ns, the initial nucleation and the early growth of martensite are

captured within the specimen. Most of the early growth products of martensite are on the annealing twin boundaries.

ACKNOWLEDGMENTS

This research was supported by the U. S. Army Research Initiative Program on Dynamic Performance of Materials (Contract DAA L-03-86-0169) and by the Lawrence Livermore National Laboratory (Contract B089339). The support and encouragement provided by Dr. L. E. Tanner, as well as discussions with Prof. G. B. Olson (Northwestern University) are gratefully acknowledged. Dr. J. C. Shyne (Stanford University) kindly provided the alloy; Dr. M. Staker (U. S. Army Materials Technology Laboratory) cold-rolled it.

REFERENCES

1. J. R. Patel and M. Cohen, Acta Met., 1 (1953) 531.

2. M. A. Meyers and J. R. C. Guimaraes, Mater. Sci. Eng., 24 (1976) 289.

3. N. N. Thadhani and M. A. Meyers, Acta Met., 34 (1986) 1625.

4. S. N. Chang and M. A. Meyers, Acta Met., 36 (1988) 1085.

5. K. T. Ramesh, B. Altman, G. Ravichandran, and S. Nemat-Nasser, in Advances in Fracture Research, eds. K. Salama, K. Ravi-Chandra, D.M.R. Taplin, and R. Rama Rao, Pergamon Press, Vol. 1, 1989, p.811.

6. Y. Sano, "Nucleation and Growth of Martensite Induced by a Tensile Stress Pulse in Fe-31.8wt%Ni-0.020wt%C Alloy," M.Sc. Thesis, UCSD, La Jolla, CA, 1990.

7. C. L. Magee, in "Phase Transformations", ASM, 1970, p.115.

8. R. B. G. Yeo, Trans. ASM 57 (1964) 48.

9. J. F. Breedis, Trans. AIME 230 (1964) 1583.

10. J. B. Oblak and B. H. Kear, Pro. 28th Annual Meeting of EMSA, 1970, p 432.

11. M. A. Meyers and L. E. Murr, Acta Met., 26 (1978) 851.

12. G. B. Olson and M. Cohen, in "Frontiers in Materials Technologies", eds. M. A. Meyers and O. T. Inal, Elsevier, Amsterdam, 1985, p3.

Figures

Figure 1 Schematic representation of target assembly.

Figure 2 Distance versus time plot when a momentum trap is used to capture a part of the tensile pulse; reduction in tensile pulse duration can seen.

Figure 3 Cross section of target showing concentration of martensite in central portion, where tensile pulse amplitude and duration are maximum.

Figure 4 Micrographs of cross sections of recovered specimens impacted with tensile pulse durations of (a) 80ns and (b) 105ns (arrows indicate incompletely grown lenses formed along boundaries).

Figure 5 (a) and (b) Micrographs showing partially grown martensite lenses in the target impacted at 105ns.

Figure 6 (a) Micrographs showing the transformation region where fully and partially grown martensites co-exist; (b) magnified region of (a); (specimen was impacted with tensile pulse duration of 105ns).

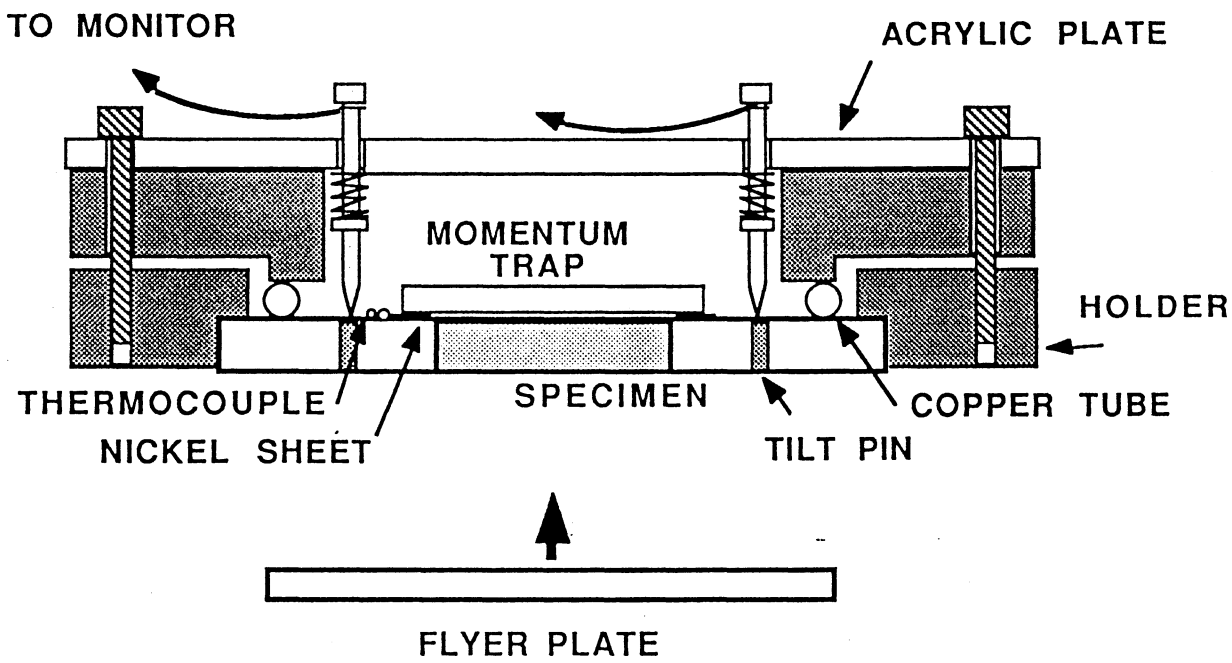

Figure 1 Schematic representation of target assembly.

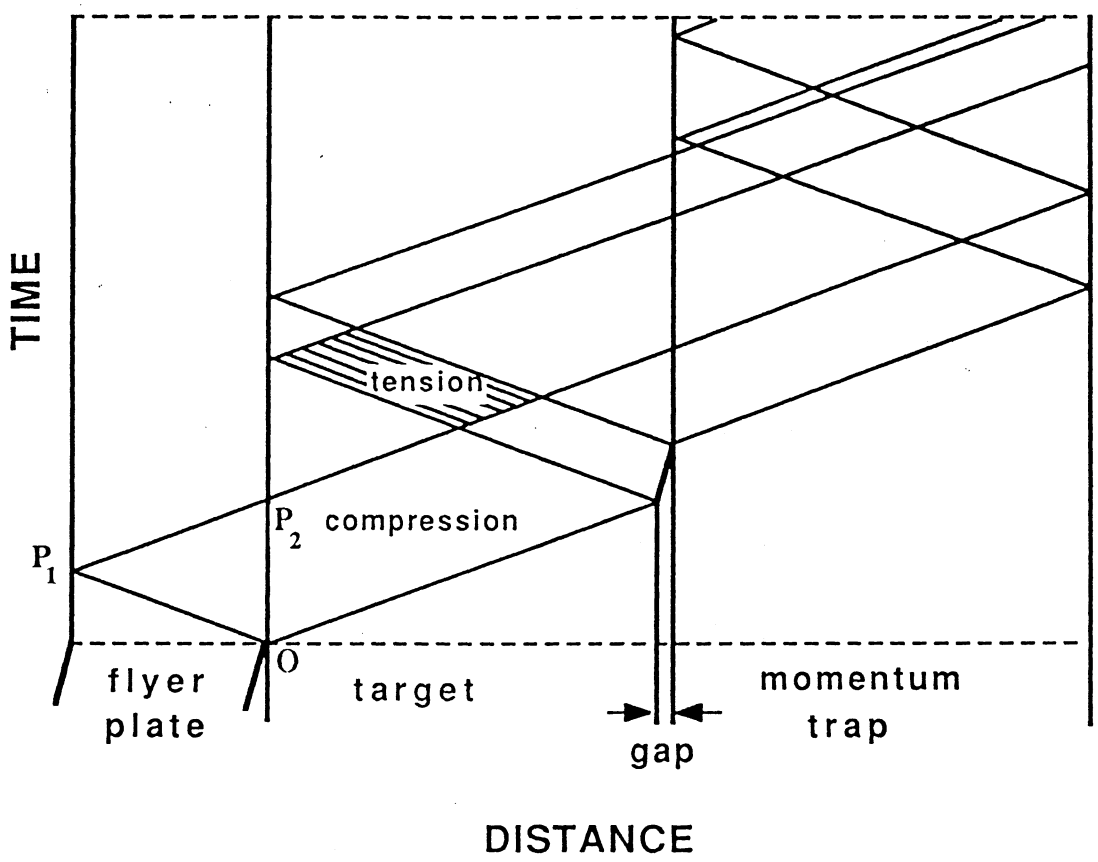

Figure 2 Distance versus time plot when a momentum trap is used to capture a part of the tensile pulse: reduction in tensile pulse duration can seen.

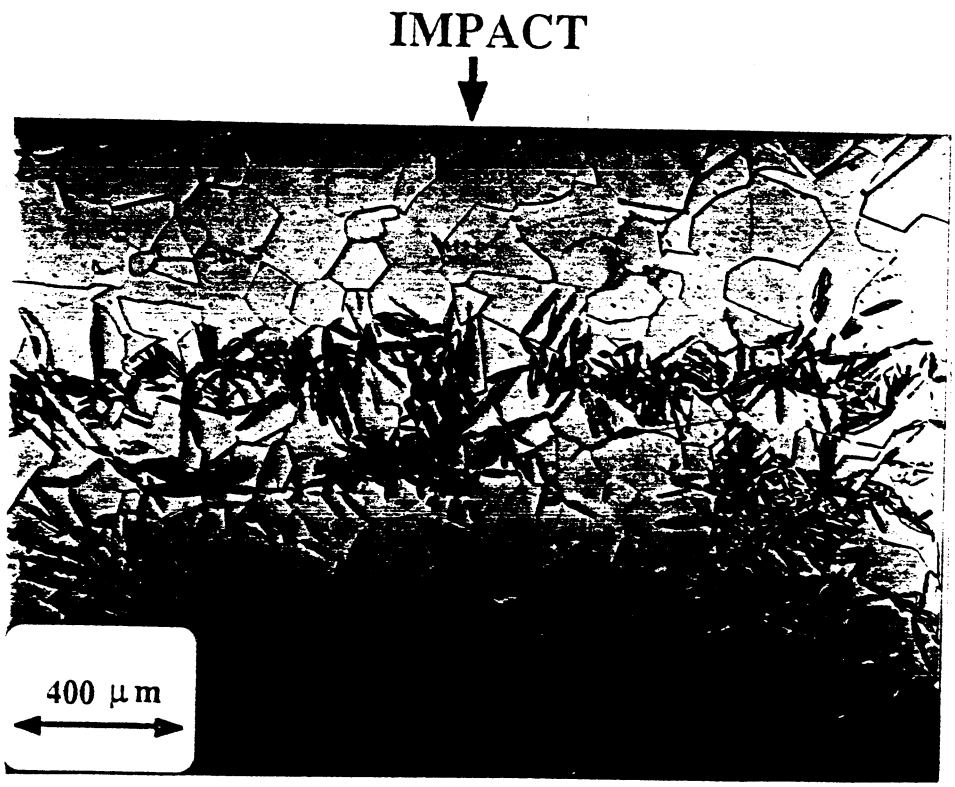

Figure 3 Cross section of target showing concentration of martensite in central portion, where tensile pulse amplitude and duration are maximum.

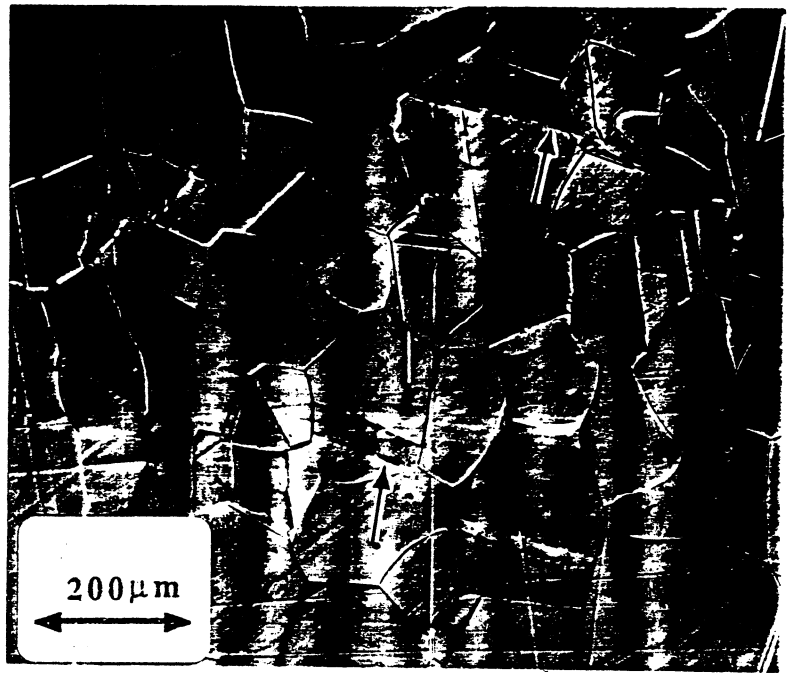

a

b

Figure 4 Micrographs of cross sections of recovered specimens impacted with tensile pulse durations of (a) 80ns and (b) 105ns (arrows indicate incompletely grown lenses formed along boundaries).

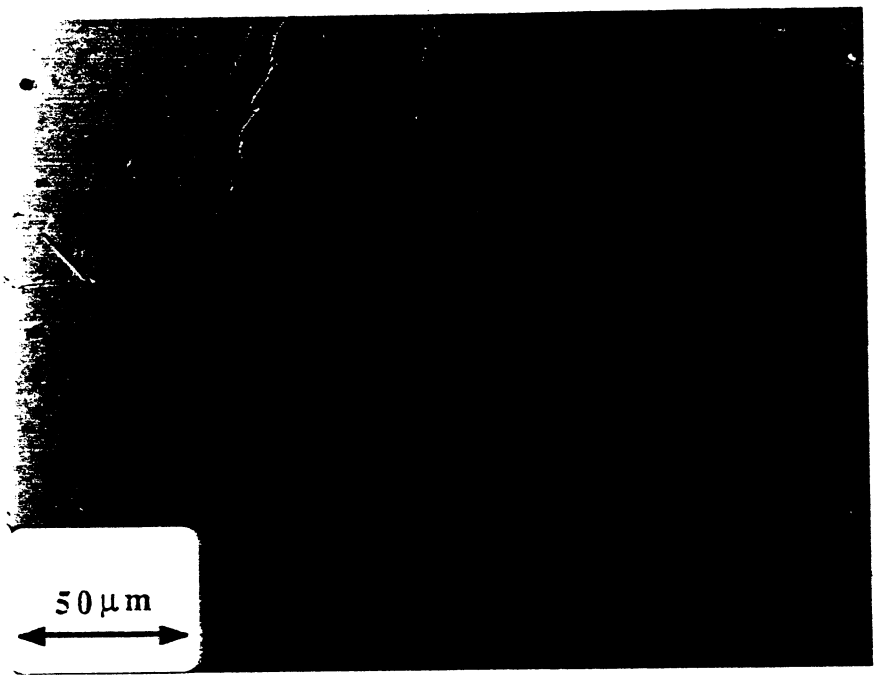

a

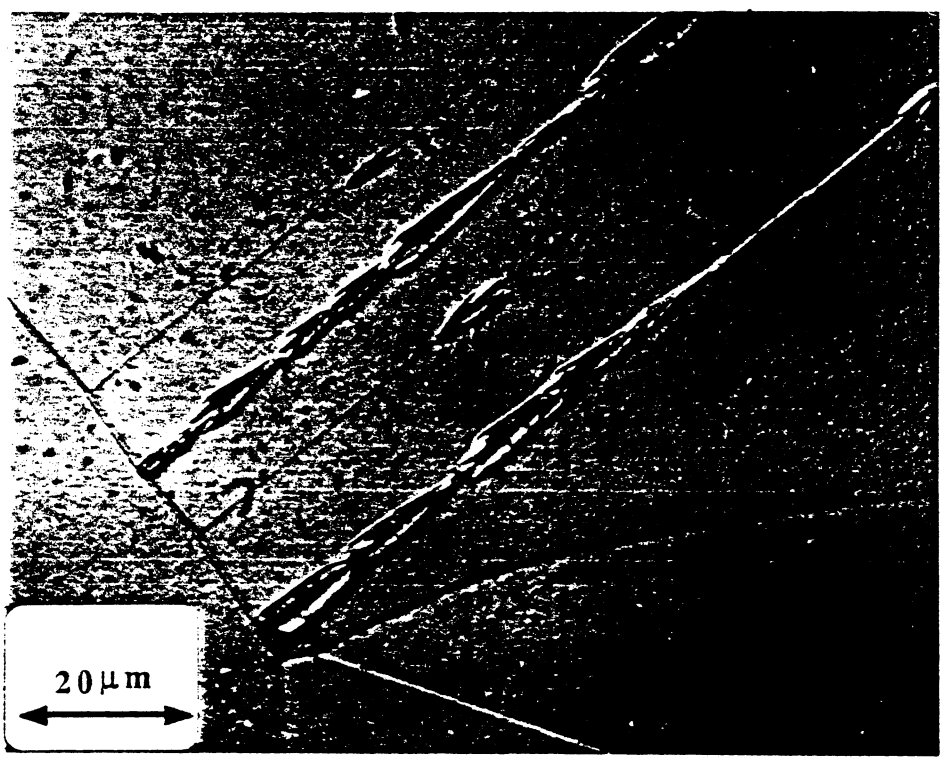

b

Figure 5 (a) and (b) Micrographs showing partially grown martensite lenses in the target impacted at 105ns.

a

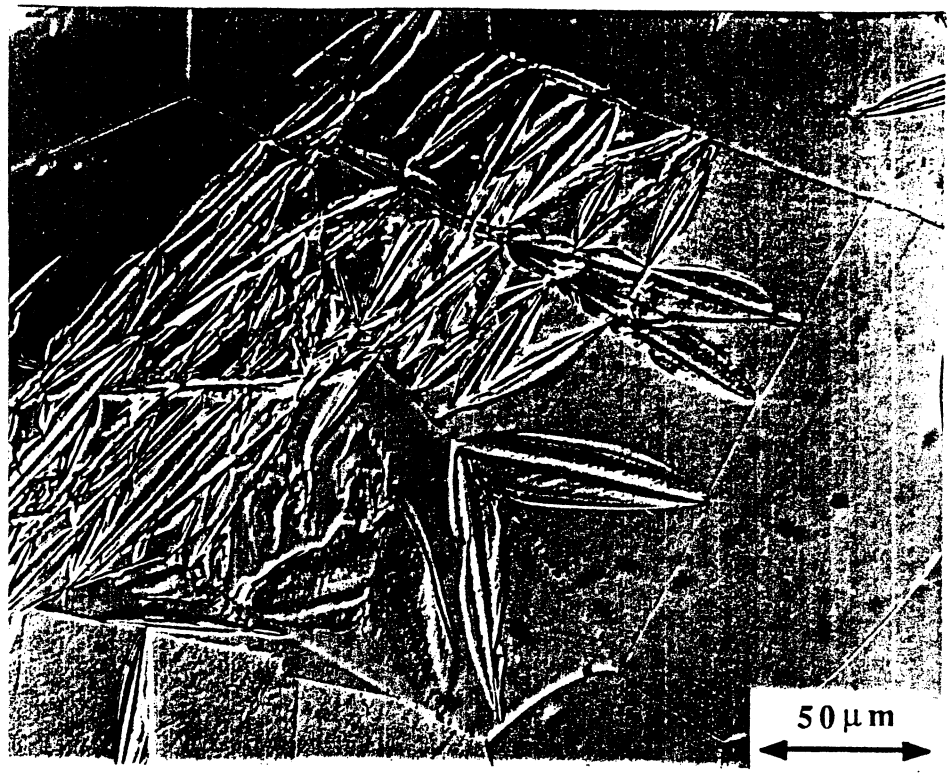

b

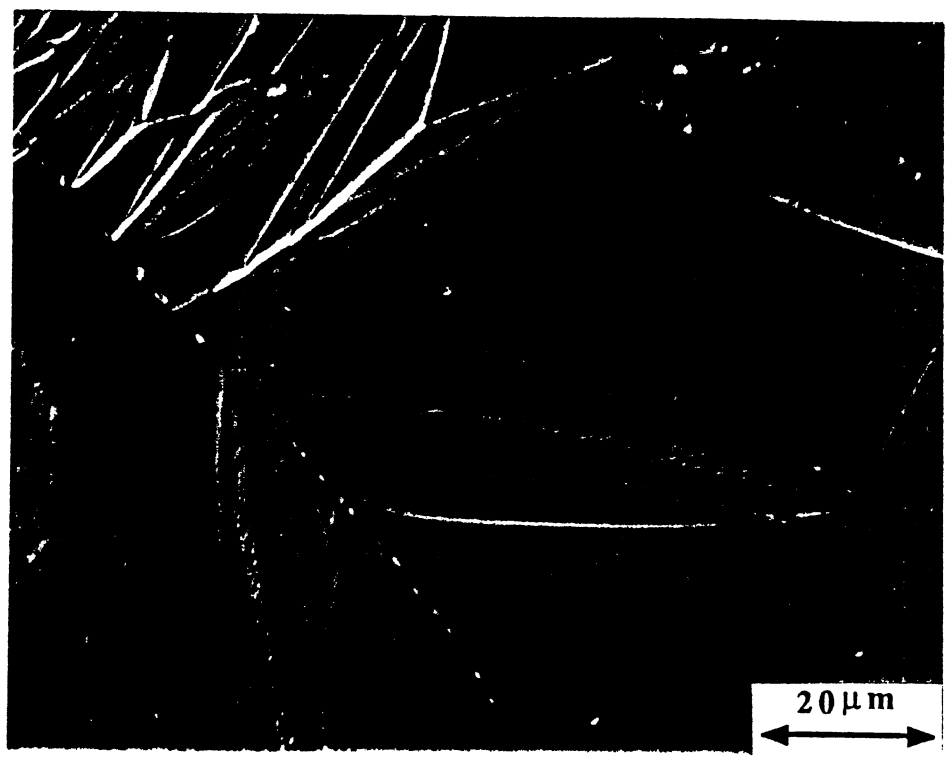

Figure 6 (a) Micrographs showing the transformation region where fully and partially grown martensites co-exist; (b) magnified region of (a); (specimen was impacted with tensile pulse duration of 105ns).

TABLE 1

Experimental Conditions for Experiments

setup	shot #	thickness (mm)		gap (μm)	impact velocity (m/s)	stress level (GPa)	tensile pulse duration (ns)	observation
		flyer	specimen					
I	1	0.6	1.6	N/A	78.6	1.4	190	no transformation
	2	0.8	1.7	N/A	90.5	1.6	245	grown plates and few frozen - inplates
II	3	0.8	1.5	10	97.5	1.7	105	fully grown plates, frozen-inplates,
	4	0.8	1.6	7.5	96.7	1.7	80	only frozen-inplates

Impact Temperature; -30°C